ZnS Deposition on Oxadiazole–Terpyridine Copolymer

A. Chrissanthopoulos, N. P. Tzanetos, A. K. Andreopoulou, J. Kallitsis, E. Dalas

Department of Chemistry, University of Patras, Patras, Greece

Received 22 September 2005; accepted 29 October 2005
DOI 10.1002/app.23656
Published online in Wiley InterScience (www.interscience.wiley.com).

ABSTRACT: The combination of inorganic salts and macromolecules leads to supramolecular structures with new interesting physical and chemical properties. The deposition of ZnS (Wurtzite) on oxadiazole–terpyridine copolymer P-90/10 synthesized by free radical copolymerization were investigated. The apparent order of the crystallization process was found to be 2 that indicated a surface diffusion-controlled mechanism. Critical nucleus formation proceeds via complexation of the ZnS molecules to the —N— atoms as concluded from computational chemistry calculations. The number of ions forming the critical nucleus was found experimentally to be ($n^*_{exp} = 1.71 \pm 0.24$) in accordance with the computational chemistry calculations by the PM3 method of the MOPAC program package. The surface energy of the growing ZnS phase was found to be 121 mJ/m^2 typical for sparingly soluble salts. © 2006 Wiley Periodicals, Inc. J Appl Polym Sci 101: 1913–1918, 2006

Key words: crystallization; molecular modeling; nucleation; functionalization of polymers; metal–polymer complexes

INTRODUCTION

ZnS is an excellent optical transmissive material because of its board band transmission (starting from 0.4 μm in the visible to about 14 μm in the infrared), a high value of refractive index, good stability, and low scatter. This material is used as windows and domes for laser, thermal imaging system, infrared detectors and sensors,[1] for the photocatalytic degradation of water pollutants,[2] as well as for light emission diodes and photovoltaic cells.[3]

The combination of inorganic salts and macromolecules leads to supramolecular structures with new interesting physical and chemical properties.[4] Also polymers containing functional groups have been found to nucleate sparingly soluble salts.[5] Results obtained by using a number of polymeric substrates were explained by the assumption that the nucleation of a crystalline salt on a polymer preceded by the formation of surface ion pairs.[6,7] Specifically, the combination of ZnS along with copolymers consisting of hole-transporting and electron-transporting segments are currently of interest because of their potential application in optoelectronic devices, photovoltaic devices, bipolar charge transport materials for light emitting diodes, lasers, and other applications.[3,4]

Increasingly computer simulation techniques based on high-quality interatomic potentials are enabling new insight in fundamental problems in nucleation and crystal growth of a wide variety of materials.[7,8] Semiempirical level of molecular orbital (MO) theory, developed under the Hartee-Fock theory using various approximations,[9] provides a useful tool to understand/predict the chemical properties of moderate size molecules.

In the present work, ZnS was precipitated on oxadiazole–terpyridine copolymer, and we have attempted to explore the mechanism of ZnS nucleation on the polymeric substrate by the PM3/MOPAC simulation method.

EXPERIMENTAL

Preparation and characterization of the polymer substrate

Materials

Monomers I and II (Fig. 1) were synthesized according to known procedures.[10,11] Azobis(isobutyronitrile) (AIBN) was recrystallized from methanol and stored in the freezer. All the other chemicals and solvents were used as received from Aldrich (Steinheim, Germany). The polymerization reaction was carried out under an argon atmosphere.

Instrumentation

IR spectra were recorded on a Perkin–Elmer 16PC FTIR spectrometer with KBr pellets. ^{1}H NMR spectroscopy measurements were performed using a Bruker Avance DPX 400MHz spectrometer. Molecular weights (M_n and M_w) were determined by gel perme-

Correspondence to: E. Dalas (vdal@chemistry.upatras.gr).

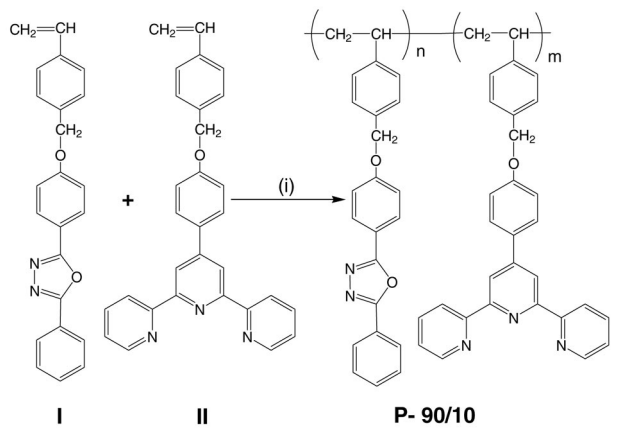

Figure 1 Free radical copolymerization of the monomer I with the monomer II and AIBN the initiator. (i): AIBN, DMF.

ation chromatography using two Ultrastyragel columns of 500 and 10^4 Å pore sizes, respectively, a UV detector, $CHCl_3$ as eluent (analytical grade), which was filtered through a 0.5 μm millipore filter, a flow rate of 1 mL/min at room temperature and calibrated using polystyrene standards. The sample was passed through a 0.2 μm millipore filter. The UV–visible absorption spectra were recorded on a Hewlett-Packard 8452 A Diode Array UV–Visible Spectrophotometer.

Free-radical copolymerization of monomers I and II

A solution of oxadiazole monomer I (1.10 g, 3.11 mmol), terpyridine monomer II (0.152 g, 0.345 mmol), and AIBN (11.33 mg, 2% mol of monomers) in dry DMF (5.5 mL) was degassed three times and flushed with argon. The mixture was heated under stirring in a sealed tube for 3 days. After cooling to room temperature, $CHCl_3$ (5–10 mL) was added to the reaction mixture to dissolve the copolymer. The copolymer was precipitated in a large excess of methanol (20-fold excess by volume) and further purified by reprecipitation from $CHCl_3$ into ethyl acetate. Thus, the obtained white solid was dried under vacuum at room temperature. Yield 1.04 g (83.07%); ^{1}H NMR ($CDCl_3$): 1.25–1.7 (two broad, CH_2CH) 4.9 (broad, OCH_2); 6.6–6.8 (broad, Oxadiazole-$C_{Ar}H$); 6.91 (broad, $CH_2CHC_{Ar}HCH_2O$); 7.18–7.4 (m broad, Oxadiazole-Terpyridine $C_{Ar}H$); 7.71 (single, Terpyridine $C_{Ar}H$); 7.9 (d broad, Oxadiazole-$C_{Ar}H$); 8.6 ppm (broad, Terpyridine-$C_{Ar}H$).

Monomer and polymer synthesis

Among the various techniques to polymerize vinyl monomers the most widely used still remains the free radical polymerization. This technique requires mild reaction conditions and is suitable for a wide range of functional monomers. These features make it suitable for both industry and research laboratories. Figure 1 shows the chemical structures of the monomers and copolymer synthesized in this study. Free radical polymerization with AIBN as the initiator was utilized for the copolymerization of the monomer I with the monomer II. The unreacted monomers were effectively removed using dissolution of the reaction mixture and precipitation in a good solvent for the monomers (ethyl acetate for the monomers I and II). Resulting copolymer P-90/10 exhibited good solubility in a wide range of organic solvents, including $CHCl_3$, THF, and DMF, which might be primarily because of the oxadiazole- and terpyridine-based side groups. The aforementioned copolymer was characterized by means of ^{1}H NMR and UV–vis spectroscopies (Fig. 2). The homogeneity of the copolymer was assessed by gel permeation chromatography based on calibration with polystyrene standards, revealing an M_n of 14,000, a polydispersity of 2.7, and a terpyridine content of 9.9% calculated from ^{1}H NMR spectrum based on the protons at 4.9 and 8.6 ppm of monomers I and II and of monomer II, respectively. Chromatograms were recorded at the standard 254 nm (detects aromatic nu-

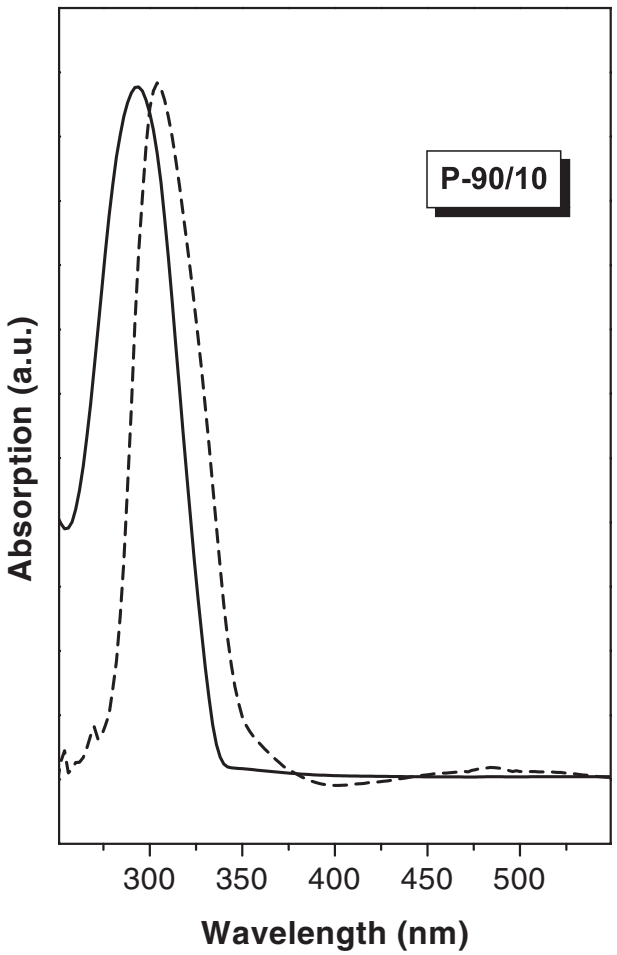

Figure 2 UV absorption spectra of polymer P-90/10 in $CHCl_3$ solution (solid line) and in film form (dashed line).

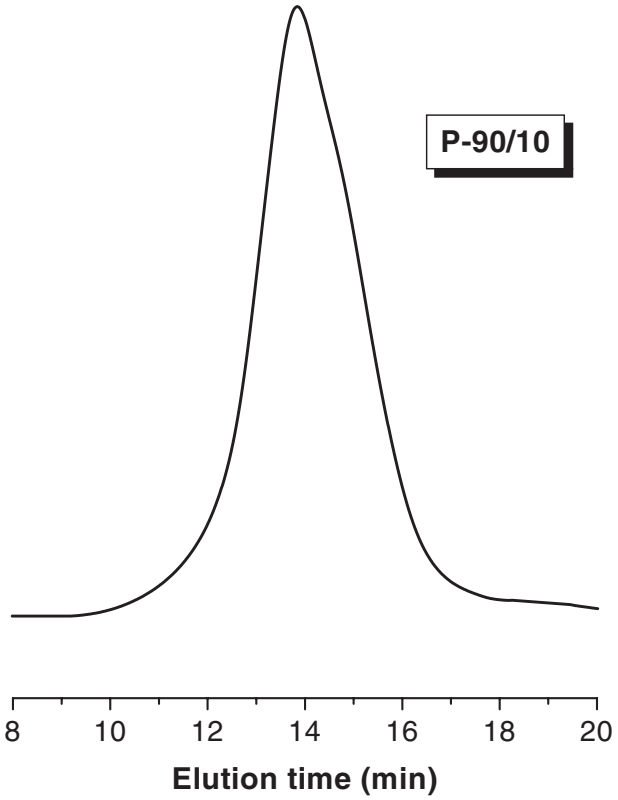

Figure 3 GPC chromatograph of copolymer P-90/10 in $CHCl_3$ detected at 254 nm.

clei). Gel permeation chromatography was also used to make sure that no traces of unreacted monomers remained in the copolymer. GPC does not reveal residual monomers (Fig. 3).

Crystallization experiments

Crystallization of zinc sulfide was done at 25°C in a 600-mL, double-walled Pyrex vessel thermostated by circulating water from a thermostat, zinc nitrate $Zn(NO_3)_2$. $4H_2O$ (Merck, proanalysi) and ammonium sulfide $(NH_4)_2S$ (Ferak, zur analyze) were used for the preparation of the respective stock solutions with triply distilled, carbon dioxide free water. Zinc solutions were standardized by atomic absorption spectroscopy (Varian 1200) and the sulfide solutions by the iodine method.[12] Then 250 mL of each of the zinc and sulfide solutions, prepared from the stock solutions, was mixed in the reactor and the solution pH was adjusted to 2.5 by the addition of standard hydrochloric acid (Merck, Titrisol), and the stability of both solution conductivity and pH was verified for over a 1 h period of time.[5] Homogeneity of the species concentration and of the solids dispersion was achieved by magnetic stirring at ~350 rpm. Following the pH adjustment in the supersaturated solution and the verification of its stability, 50 mg of exactly weighted copolymer P-90/10 was suspended in the supersaturated solution. The specific surface area of the copolymer powder determined by nitrogen adsorption (multiple point BET, Perkin-Elmer Model 212D sorptometer) was 16.2 m^2/g. Upon introduction of the copolymer powder into the supersaturated solutions the precipitation started immediately, accompanied by changes in pH and conductivity of the solution.[3,5] During the course of the precipitation process, samples were withdrawn and filtered through membrane filters (Millipore 0.1 μm) and the liquid phase was analyzed for zinc by atomic adsorption spectrometry. The rates of precipitation were computed as initial rates from the slopes of the zinc concentration versus time data, and they were normalized per unit surface area of the polymer substrate. The rates measured were very reproducible better than 5% (a mean of five experiments). The solid phases formed during the course of precipitation were examined by FTIR spectroscopy (Perkin-Elmer 16-PC FTIR using KBr pellets), powder X-ray diffraction (Phillips, 1300/00, Cukα radiation), and scanning electron microscopy (JEOL JSM 5200), with an energy dispersive X-ray microprobe (EDXS) and LEO supra 35 VP.

RESULTS AND DISCUSSION

Examination of the precipitated solids by (a) X-ray diffraction reveals the characteristic reflections of Wurtzite[13] with *d*-spacing 3.120, 1.904, 1.626, *hkl* (0010), (110), (1110), and intensities 90, 52, 34, respectively; (b) scanning electron microscopy (Fig. 4) and (c) EDS microanalysis (Fig. 5) confirmed the exclusive formation of ZnS (Wurtzite). Similar spherulitic morphology for ZnS was obtained by homogeneous precipitation from acidic zinc salt solutions.[14]

The solution speciation in all experiments was computed by the HYDRAQL program, from the pH, the

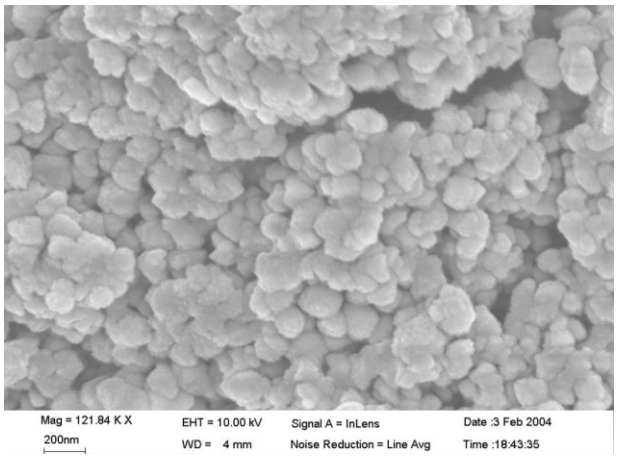

Figure 4 Scanning electron micrograph of ZnS precipitated on the copolymer P-90/10.

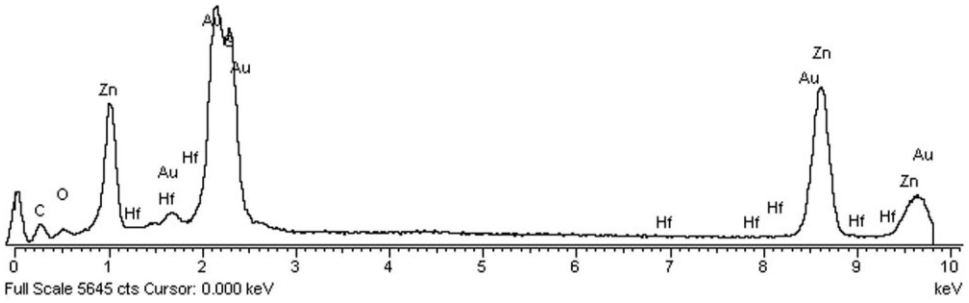

Figure 5 EDS surface microanalysis of ZnS precipitated on copolymer P-90/10.

total mass balance, the ion pair formation for zinc and sulfur, and the electroneutrality conditions.[15,16] The activity coefficients were calculated from the extended Debye-Hückel equation corrected for ion interactions. The driving force for the crystal growth of ZnS is the difference $\Delta\mu$ in the chemical potentials $\mu_{\text{supersat.}}$, in the supersaturated solution, and at equilibrium, $\mu_{\text{eq.}}$

$$\Delta G = \mu_{\text{eq.}} - \mu_{\text{supersat.}} \tag{1}$$

since

$$ZnS = Zn^{2+} + S^{2-} \tag{2}$$

$$\mu_{\text{supersat.}} = \mu_{Zn^{2+}} + \mu_{S^{2-}}$$

$$\mu_{\text{supersat.}} = \mu^0 + RT\ln[(Zn^{2+})(S^{2-})]^{1/2} \tag{3}$$

In eq. (3), parentheses denote the activities of the corresponding ions, R is the gas constant and T is the absolute temperature. Similarly, at equilibrium

$$\mu_{\text{eq.}} = \mu^0 + RT\ln[(Zn^{2+})_{\text{eq.}}(S^{2-})_{\text{eq.}}]^{1/2}$$

$$\mu_{\text{eq.}} = \mu^0 + RT\ln[K^0_{ZnS}]^{1/2} \tag{4}$$

From eqs. (1), (2), and (4), it follows that

$$\Delta\mu = -RT\ln\left[\frac{(Zn^{2+})(S^{2-})}{K^0_{ZnS}}\right]^{1/2} \tag{5}$$

$$\Delta\mu = -\frac{1}{2}RT\ln\Omega \tag{6}$$

In eq. (6), Ω is the supersaturation ratio with respect to ZnS, K^0_{ZnS} is the thermodynamic solubility product of ZnS (1.230×10^{-22}), and σ is the relative supersaturation:

$$\sigma = \Omega^{1/2} - 1 \tag{7}$$

and the mean free energy change per mole of ions shall then be

$$\Delta G = -(RT/2)\ln\Omega \tag{8}$$

The initial conditions and the measured rates are shown in Table I. Doubling or tripling the amounts of copolymer introduced in the supersaturated solution had no effect on the initial rates normalized per unit surface area of the substrate. Also changes in the stirring rate (between 60 and 350 rpm) had no effect on the measured crystallization rate. It may, therefore, be suggested that zinc sulfide overgrowth was induced by the copolymer P-90/100 by heterogeneous nucleation.[17]

The size of the critical nucleus may be estimated from the slope of the plots of the logarithm of the initial rates, R, as a function of the logarithm of the initial zinc concentration.[18]

$$\frac{d\ln R}{d\ln[Zn^{2+}]_0} = n^*_{\text{exp.}} \tag{9}$$

In Figure 6 such a plot is shown and a value $n_{\text{exp.}} = 1.71 \pm 0.24$ was obtained from the slope of the curve ln R against $\ln[Zn^{2+}]_0$.

The Parametric Method 3 (PM3)[19] included in the version 6.0 of MOPAC program package[20] was used for the computational chemistry calculations for the nucleation process. This method that is based on the neglect of diatomic differential overlap (NDDO) formation employs an s-p basis set and does not include d orbitals. It has been reported[21] that it has mean unsigned errors in molecular geometries of 0.036 Å (bond lengths), 3.93° (angles), and 14.9° (torsion angles). The geometries were fully optimized in Carte-

TABLE I
Crystal Growth of ZnS on P-90/100 Copolymer[a]

Zn_t (10^{-4} M)	ΔG_{ZnS} (kJ/mol[1)]	R (10^{-7}mol/min m^2)
1	−19.341	6.57
0.75	−19.236	2.91
0.5	−18.396	1.30
0.25	−17.220	0.58

[a] Total zinc, Zn_t = total sulfide, S_t; pH 2.5; 25°C; 0.1 mg copolymer/ml.

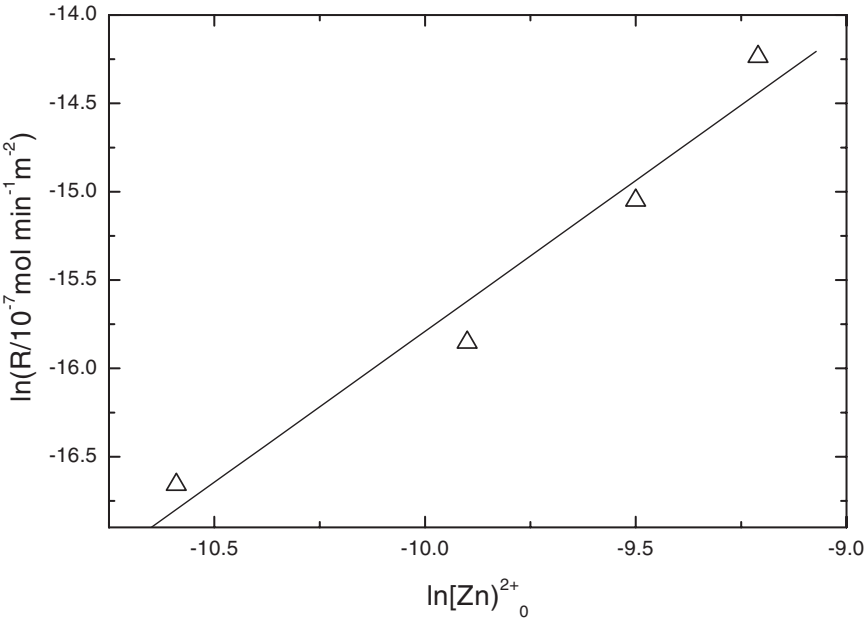

Figure 6 Initial rate of the deposition of ZnS on copolymer P-90/10 as a function of the initial zinc concentration in solution [eq. (9)].

sian coordinates (*XYZ*) using the BFGS method or the Eigenvector following routine (EF). The final geometry corresponds to a stationary point on the potential surface and this is one of many possible conformations. To apply a MO method to macromolecules such as polymers, we simulate the long chain polymeric structure by finite models-oligomers, having terminal hydrogens.

We first optimized the structure (geometry) of the molecular model and evaluated the polymer's heat of formation as well as the heat of formation of the $(ZnS)_n$ molecules. The next step was to find the active sites of the polymer having the property to bound the $(ZnS)_n$ molecules. These are the nitrogen atoms of the polymer chains and the most active among them is the nitrogen of the pyridine assigned as active site 2 (Fig. 7). The value of $n = 1$–3 depends on the active site where the nucleation process takes place as schematically shown in Figure 7.

We calculate subsequently the energy difference (ΔE) between the isolated molecules [polymer and $(ZnS)_n$] and the polymer–zinc sulfide complexes, according to eq. (10), to have a measure of the ability of the system to stabilize these forms (Table II).

$$\Delta E = \Delta H_{f,298}(\text{polymer}.n\text{ZnS}) - [\Delta H_{f,298(\text{polymer})} + \Delta H_{f,298}(\text{ZnS})_n \quad (10)$$

We also calculated the bond order between zinc and nitrogen atoms, the active site's nitrogen partial charge and the $(ZnS)_n$ charge in the complexes as a sum of zinc and sulfur atom charges. Finally, 1–3ZnS molecules were introduced at a distance of about 4 Å from the polymer's more active site and the system was let free its equilibrium position. At the optimized geometry, the coordination number of ZnS molecules around nitrogen is 1. The zinc atoms are located at a distance of ~2.1 Å, having a bond order equal to ~0.6. The addition of more than one zinc sulfide molecules results in the formation of $(ZnS)_n$ complexes binding to nitrogen active site via a N—Zn bond. In Table II, the energies of formation, the bond order, and the charges are presented. From this table, it is obvious that an electron density (or negative charge) was moved from the pyridine rings to zinc sulfide bonded

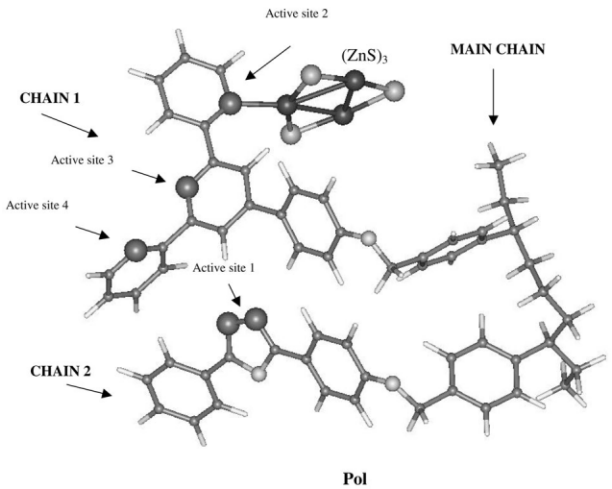

Figure 7 Ball and stick draw of the ZnS cluster-copolymer P-90/10 structure.

TABLE II
MOPAC/PM3 Calculated Properties of the Oligomer-Model, $(ZnS)_n$ and Their Complexes

	$\Delta H_{f,298}$ (K cal/mol)	ΔH (K cal/mol)	N—Zn bond order	Nitrogen charge	ZnS charge
Pol	120.6			−0.07	
ZnS	51.5				
$(ZnS)_2$	−39.6	−32.0	0.76		−0.58
$(ZnS)_3$	−125.7	−21.5	0.70	0.39	−0.58
[Pol] ZnS	140.1	−15.7	0.63	0.34	−0.50
[Pol] $(ZnS)_2$	59.5			0.30	
[Pol] $(ZnS)_3$	−20.9				

to the polymer, resulting in a red shift (lower E_g values) in absorption maxima of the final obtained polymer–ZnS supramolecular structure.[4,22,23] As shown in Figure 7, the complexation of ZnS molecules around the —N— atoms of the polymer with $n^* = 1$–3 (depending on the active growth site where the nucleation takes place) is a possible mechanism for the critical nucleus formation. Also this value determined from theoretical calculations is quite close to the experimentally obtained $n^*_{exp.} = 1.71 \pm 0.24$ from eq. (9) applied in homogeneous nucleation processes.[17,18]

An estimate for the surface energy γ of the ZnS overgrowth may be obtained from the dependence of the initial rate of the precipitation on the inverse of the squared logarithm of the solution supersaturation according to the equation:[17]

$$R = \ln B - \frac{\Phi\beta\gamma^3 u^2}{k^3 T^3} \frac{1}{(\ln\Omega)^2} \qquad (11)$$

In eq. (11), B is a constant, u is the molecular volume ($d_x = 4.104$ g/cm^3) of the growing phase,[13] k is the Boltzmann constant, β is the shape factor, and T is the absolute temperature. From the slope of the line, a value of 121 mJ/m^2 was obtained for the $\gamma\Phi$ of the growing zinc sulfide on the copolymer P-90/10 assuming spherical shape nuclei $\beta = 16.76$. In eq. (12) Φ is a factor expressing the compatibility between the salt formed and the polymer substrate and is given by $\Phi = (2 + \cos\theta)(1 - \cos\theta)^2/4$, where θ is the contact angle. The theoretical value for the surface energy of ZnS calculated from the nucleation theory[18,24] was 750 mJ/m^2. To have agreement for the surface energy of the overgrowing zinc sulfide Φ must be equal to 0.161. Logarithmic plots of the rates of ZnS formation on the copolymer P-90/10, R, as a function of the relative solution supersaturation, σ, yielded a straight line from the slope from which an apparent order $n = 2.49 \pm 0.59$ was calculated, which may be interpreted as indicative of a surface diffusion controlled mechanism.[25]

In conclusion, it can be said that the copolymer P-90/10 tested in this work stabilize the formation of Wurtzite (ZnS). Critical nucleus formation proceed via complexation of the ZnS molecules to the —N— atoms of the polymer as concluded from computational chemistry calculations with $n^* = 1$–3 and $n^*_{exp.} = 1.71 \pm 0.24$. Also there is an electron density movement from the pyridine rings to zinc sulfide. The surface energy of the growing ZnS phase was $\gamma = 121$ mJ/m^2 and the apparent order of the crystallization process $n = 2.49 \pm 0.59$ indicated a surface diffusion controlled mechanism.

References

1. Tran, N. H.; Lanb, R. N.; Mar, G. L. Colloids Surf A 1999, 155, 93.
2. Kho, R.; Torres-Martinez, C. L.; Mehra, K. J Colloid Interface Sci 2000, 227, 561.
3. Tsamouras, D.; Dalas, E.; Sakkopoulos, S.; Koutsoukos, P. G. Langmuir 1998, 14, 5298.
4. Gong, X.; Ng, P. K.; Chan, W. K. Adv Mater 1998, 10, 1337.
5. Dalas, E.; Sakkopoulos, S.; Kallitsis, J.; Vitoratos, E.; Koutsoukos, P. G. Langmuir 1990, 6, 1356.
6. Dalas, E.; Kallitsis, J.; Koutsoukos, P. G. Langmuir 1991, 7, 1822.
7. Malkaj, P.; Chrissanthopoulos, A.; Dalas, E. J Crystal Growth 2002, 242, 233.
8. Dalas, E.; Chrissanthopoulos, A. J Crystal Growth 2003, 255, 163.
9. Crammer, C. J. Essentials of Computational Chemistry; Wiley: Chichester, England, 1997.
10. Jiang, X. Z.; Register, R. A.; Killeen, K. A.; Thomson, M. E.; Pschenitzka, F.; Sturm, J. C. Chem Mater 2000, 91, 6717.
11. Jiang, X. Z.; Register, R. A.; Killeen, K. A.; Thomson, M. E.; Pschenitzka, F.; Herbner, T. R.; Sturm, J. C. J Appl Phys 2002, 91, 6717.
12. Karchnier, J. H. The Analytical Chemistry of Sulfur and Its Compounds, Part 1; Wiley: New York, 1970.
13. Joint Committee for Powder Diffraction Studies, JCPDS card file No. 12–0688, Compact Disc, 1999.
14. Eshuis, A.; van Elderen, G. R. A.; Koning, C. A. J. Colloids Surf A 1999, 151, 505.
15. Smith, R. M.; Martell, A. E. Critical Stability Constants, Vol. 4; Plenum: New York, 1976.
16. Papelis, C.; Hayes, K. F.; Leckie, J. O. A program for the computation of equilibrium composition of aqueous batch systems (Technical Report No. 306); Stanford University, Stanford, 1988.
17. Nyvlt, J.; Sohnel, P.; Matuchova, M.; Broul, M. The Kinetics of Industrial Crystallization; Pergamon: Oxford, 1985; pp 68, 284.
18. Nielsen, A. E.; Kinetics of Precipitation; Pergamon: Oxford, 1964; p 18.
19. Stewart, J. J. P. J Comput Chem 1989, 10, 209.
20. Stewart, J. J. P. QCPE Bull 1983, 3, 43.
21. Stewart, J. J. P. J Comput Chem 1989, 10, 221.
22. Heller, M.; Schuber, U. Macromol Rapid Commun 2002, 23, 411.
23. Shubert, U.; Hofmeier, H. Macromol Rapid Commun 2002, 23, 561.
24. Koutsoukos, P. G. Ph.D. Thesis, SUNYAB, 1980.
25. Nielsen, A. E. Pure Appl Chem 1981, 53, 2025.